Pergamon

Acta mater. Vol. 46, No. 2, pp. 565–577, 1998

Printed in Great Britain
PII: S1359-6454(97)00230-9
1359-6454/98 $19.00 + 0.00

FLOW STRESS OF F.C.C. POLYCRYSTALS WITH APPLICATION TO OFHC Cu

SIA NEMAT-NASSER and YULONG LI†

Center of Excellence for Advanced Materials, Department of Applied Mechanics and Engineering Sciences, University of California, San Diego, La Jolla, CA 92093-0416, U.S.A.

(Received 10 February 1997; accepted 18 July 1997)

Abstract—Based on the concept of dislocation kinematics and kinetics, paralleled with a systematic experimental investigation, a physically-based model is developed for f.c.c. polycrystals, using OFHC copper for illustration. First, the concept of the motion of dislocations and the barriers that they must overcome in their motion, is used as an underlying motivation to obtain general expressions which include a number of free constitutive parameters. These parameters are then evaluated by direct comparison with experimental data. High strain-rate compression experiments are performed using UCSD's recovery Hopkinson technique (see Nemat-Nasser, S., Isaacs, J. B. and Starrett, J. E., *Proc. R. Soc.*, 1991, **435A**,, 371; Nemat-Nasser, S., Li, Y. F. and Isaacs, J. B., *Mech. Mater.*, 1994, **17**, 111; Nemat-Nasser, S. and Isaacs, J. B., *Acta Metall.*, 1997, **45**, 907). Strains close to 100% are achieved in these tests, over a temperature range of 77–1100 K, and strain rates of 10^{-3} to 8000 s^{-1}; the quasi-static tests are performed using an Instron machine. For low-temperature tests, both the as-received and annealed samples are tested. With few free constitutive parameters, good correlation between the theoretical predictions and experimental results is obtained, over the entire range of strain rates and temperatures. The orders of magnitude of several of these parameters are first estimated based on the underlying structure of the material. Experimental results are then used to tune the final values of these parameters. It turns out that the structure of the constitutive relations and the value of a number of the constitutive parameters are essentially the same for commercially pure tantalum (b.c.c. metal) and OFHC copper. The relation between the two cases is examined and the similarities and differences are discussed. © *1998 Acta Metallurgica Inc.*

1. INTRODUCTION

Inelastic deformation of crystalline solids is, in general, rate- and temperature dependent. The classical rate-independent plasticity theories represent idealizations which, in general, have limited applicability. The rate- and temperature dependency become especially dominant for high strain-rate deformations, where adiabatic plastic flow may produce significant temperature changes in the material.

In the rate-dependent phenomenological approach, the effective plastic strain rate, $\dot{\gamma}$, is expressed in terms of the effective stress, τ, temperature, T, and some internal variables which represent the effect of the thermomechanical loading history on the current microstructure and, hence, on the response of the material. In many models for metals, the total accumulated effective plastic strain, γ, is used as the only variable representing the history effects‡. In general, however, this representation has only a limited predictive capability. Indeed, for this approach to yield useful results, it may often be necessary to evaluate the parameters in constitutive models of this kind, from experiments which are conducted at strains, strain rates, and temperatures close to the range of the values to which the model will eventually be applied.

There are models which are based on rational analysis of the underlying micrommechanisms of the inelastic response of the material. For applications, however, simplifying assumptions are generally inevitable, and these kinds of micromechanical models also eventually rely on empirical evaluation of their constitutive parameters. For metals which deform plasticity essentially through dislocation motion and accumulation, physically based models have been developed based on the notion of thermally activated dislocation kinetics, for moderate strain rates (say, less than 10^4 s^{-1}), and the notion of the dislocation–drag mechanism for deformations at greater strain rates (see, e.g., Refs [3–11]).

The motion of dislocations through the crystals of a polycrystalline alloy is a complex phenomenon with various features which cannot be described by simple mathematical models which may be necessary for implementation into large-scale computer programs. While aspects of the kinetics and kinematics of dislocation motion have been understood and modeled§ , their incorporation into tractable

†Permanent address: Northwestern Polytechnical University, Xian, People's Republic of China.

‡Since plastic strain is not a thermodynamic state variable, it is better to use the dislocation density. This, however, cannot be directly measured by simple means.

§See, e.g. Refs [12–14].

and computationally simple and practical constitutive relations is yet an unsolved problem in need of fundamental study.

This issue has recently been addressed for b.c.c. metals by Nemat-Nasser and Isaacs [3] through a systematic experimental investigation of the flow stress of commercially pure tantalum, paralleled by physically-based modeling, based on the concept of dislocation kinematics and kinetics. A similar approach is used in the present work to study OFHC copper, an f.c.c. polycrystal. In this approach, the concept of the motion of dislocations and the barriers that they must overcome in their motion, are used as an underlying motivation to obtain general expressions which include a number of free constitutive parameters. These parameters are then evaluated by direct comparison with experimental data.

High strain-rate compression experiments are performed using UCSD's recovery Hopkinson technique (see Refs [1–3]). Strains close to 100% are achieved in these tests, over a temperature range of 77–1100 K, and strain rates of 10^{-3} to $8000s^{-1}$; the quasi-static tests are performed using an Instron machine. For low-temperature tests, both as-received and annealed samples are tested. With few free constitutive parameters, good correlation between the theoretical predictions and experimental results is obtained, over the entire range of strain rates and temperatures. The orders of magnitude of several of these parameters are first estimated based on the underlying structure of the material. Experimental results are then used to tune the final values of these parameters. It turns out that the structure of the constitutive relations and the value of a number of the constitutive parameters are essentially the same for commercially pure tantalum and OFHC copper. The relationship between the two cases is examined and the similarities and differences are discussed.

2. A PHYSICALLY BASED MODEL

Plastic flow in the range of temperatures and strain rates where diffusion and creep are not dominant, occurs basically by the motion of dislocations. The flow stress, τ, therefore, is essentially defined by the material resistance to this process. The motion of dislocations is opposed by both short-range and long-range obstacles (see, e.g. Ref. [5]). The short-range barriers may be overcome by thermal activation, whereas the resistance owing to long-range obstacles is essentially independent of the temperature, i.e. it is *athermal*. The short-range barriers may include the Peierls stress (b.c.c. metals), point defects such as vacancies and self-interstitials, other dislocations which intersect the slip plane, and alloying elements and solute atoms (interstitials and substitutionals). The long-range barriers may include grain boundaries, far-field forests of dislocations, and other microstructural elements with far-field influence.

The flow stress, τ, is expressed as $\tau(\gamma, \dot{\gamma}, T) = \tau^*(\gamma, \dot{\gamma}, T) + \tau_a(\gamma)$, where τ^* and τ_a are the thermal and athermal parts of the resistance to the dislocation motion, respectively. The stress, τ^*, is a decreasing function of temperature, T, and an increasing function of strain rate, $\dot{\gamma}$. The athermal part, τ_a, increases with increasing accumulated dislocations whose elastic field hinders the motion of mobile dislocations. While this elastic field does not directly depend on the temperature, it is affected by temperature in at least two ways: (1) through the elastic moduli and their dependence on the temperature; and (2) through the effect of the temperature history on the density of far-field dislocation forests. At suitably high temperatures, metals anneal, leading to a reduction in the dislocation density and hence in the corresponding elastic stress field. It may be necessary to account for this effect of temperature history when the model is applied in high-temperature regimes. The athermal part of the flow stress is, however, independent of the strain rate, although the strain-rate history does affect the temperature history and hence the current dislocation density.

It is generally assumed that the plastic strain rate, $\dot{\gamma}$, can be written in terms of the density of the mobile dislocations, ρ_m, their average velocity, $\bar{v}$, and the magnitude of the Burgers vector, b as

$$\dot{\gamma} = b\rho_m \bar{v}, \tag{1}$$

where the average dislocation velocity, $\bar{v}$, proximated by

$$\bar{v} = d\omega_0 \exp -\Delta G/kT. \tag{2}$$

Here, d is the average distance the dislocations move between barriers, ΔG is the increment of the energy barrier which the dislocation must overcome by its thermal activation, ω_0 is the frequency of such attempts, k is the Boltzmann constant, and T is the absolute temperature. Hence it follows that

$$\begin{aligned}\dot{\gamma} &= bd\rho_m\omega_0 \exp -\Delta G/kT \\ &= \dot{\gamma}_r \exp -\Delta G/kT, \qquad \dot{\gamma}_r = bd\rho_m\omega_0.\end{aligned} \tag{3}$$

The remaining task now is to express the energy barrier, ΔG, in terms of the stress, $\tau^* = \tau - \tau_a$, and temperature, T.

Consider a power-law relation between the thermally activated flow stress, $\tau^*(\gamma, \dot{\gamma}, T)$, and the activation energy, ΔG, [5]:

$$\begin{aligned}\Delta G &= G_0\left\{1 - \left(\frac{\tau^*(\gamma, \dot{\gamma}, T)}{\hat{\tau}}\right)^p\right\}^q, \\ G_0 &= \hat{\tau} b\lambda l, \\ \hat{\tau} &= \tau^*(\gamma, \dot{\gamma}, 0)\end{aligned} \tag{4}$$

where λ and $l = d$ are the average effective barrier width and the dislocation spacing, respectively, and

$0 < p \leq 1$ and $1 \leq q \leq 2$. As is shown by Kocks *et al.*, essentially all barrier profiles of interest can be modeled by proper choice of the exponents p and q. In the present work, we follow the procedure outlined by Nemat-Nasser and Isaacs [3], and establish these exponents experimentally. It turns out that $p = 2/3$ and $q = 2$ are suitable values for dislocations as barriers†.

In equation (4), $\hat{\tau}$ is the shear stress above which the barrier is crossed by a dislocation without any assistance from thermal activation. In view of equation $(4)_2$, for dislocations as barriers, $\hat{\tau}$ is inversely proportional to the average dislocation spacing, l, and hence will depend on the current dislocation density. This is a feature which distinguishes copper, an f.c.c. crystal, from tantalum, a b.c.c. crystal.

From equations (3) and (4), it now follows that

$$\tau^*(\dot{\gamma}, \gamma, T) = \left\{\hat{\tau}\left[1 - \left(-\frac{kT}{G_0}\ln\frac{\dot{\gamma}}{\dot{\gamma}_r}\right)^{1/q}\right]^{1/p}\right\}$$

$$\text{for } T \leq T_c = 0 \text{ for } T > T_c, \tag{5}$$

where, as will be shown in the sequel, $\dot{\gamma}_r$ depends on the plastic strain, γ, for the dislocations as barriers, and T_c is a critical temperature above which the dislocations can overcome their barriers by their own thermal activation. In the case of dislocations as barriers, this critical temperature will depend on the plastic strain‡, as well as on the strain rate.

2.1. *Effect on accumulated dislocations*

From equation $(4)_2$, $\hat{\tau}$ is given by

$$\hat{\tau} = \frac{G_0}{V*} = \frac{G_0}{b\lambda l}. \tag{6}$$

Here, b is a constant and λ is dependent on the profile of the barrier. The distance l, on the other hand, directly depends on the density of dislocations and hence on the plastic strain history, if the dislocations which intersect the slip planes are actually the barriers to the motion of mobile dislocations which are lying on the slip planes. For the Peierls barriers, both λ and l are of the order of the lattice dimensions; l is constant and λ may be interpreted as an effective average width of the barrier. Many b.c.c. crystals are assumed to possess this feature. This is the model used by Nemat-Nasser and Isaacs [3] for commercially pure tantalum. For f.c.c. crystals, on the other hand, the energy required to cross the Peierls barrier is generally rather small (less than 0.2 eV), so that only at very low temperatures does the Peierls mechanism provide significant resistance to the dislocation motion. In this case, the dislocation forests which intersect the slip planes are the essential barriers to the motion of the dislocations lying on the slip planes. This is the case considered in the sequel.

The average spacing, l, of the dislocation forests (barriers) along a mobile dislocation line, and the average distance, d, a mobile dislocation travels before encountering the next dislocation barrier, are basically the same, relating to the current density of the dislocations, ρ_c, by

$$l = d \approx \rho_c^{-1/2}, \tag{7}$$

where the subscript c in ρ_c denotes the current existing dislocations.

In general, the current density of dislocations, ρ_c, does not directly relate to the accumulated plastic deformation, γ, which is the result of the motion of all mobile dislocations throughout the entire history of the plastic flow. Indeed, even after extensive plastic flow, at relatively high temperatures, ρ_c may be rather small owing to the annealing that may take place at elevated temperatures. Hence, in actuality, both plastic strain and temperature histories must be considered in estimating the average current dislocation density, ρ_c, and hence the average dislocation spacing, l.

In the present case, we consider a simple empirical model, and assume that the average dislocation spacing is a decreasing function of the accumulated plastic strain and an increasing function of temperature, writing

$$l = d = \frac{l_0}{f(\gamma, T)}, \quad f(\gamma, T) > 0, \quad f(0, T_0) = 1$$

$$\frac{\partial f(\gamma, T)}{\partial \gamma} \geq 0, \quad \frac{\partial f(\gamma, T)}{\partial T} \leq 0, \tag{8a}$$

where f is some nondecreasing dimensionless function of the plastic strain, γ, and a nonincreasing function of temperature, T; T_0 is the initial temperature; and l_0 is the initial average dislocation spacing. As an illustration, consider

$$l = \frac{l_0}{1 + a(T)\gamma^{n_0}}, \quad a(T), n_0 \geq 0, \quad \frac{\partial a(T)}{\partial T} \leq 0. \tag{8b}$$

With constant a, this leads to a strain-hardening similar to that of the Johnson and Cook model [16] (1983). Here, $a(T)$ and n_0 are viewed as adjustable constitutive parameters, with n_0 between 0 and 1, and the functional form of $a(T)$ to be established empirically. Since workhardening is associated with the increasing dislocation density and, hence, with the decreasing average dislocation spacing, the function $a(T)$ is assumed to be non-negative. Furthermore, since the density of dislocations is

†These are the same values used by Nemat-Nasser and Isaacs [3] to model the flow stress of the commercially pure tantalum (b.c.c. metal) over a broad range of temperatures, strains, and strain rates. Ono [15] suggests that these values of q and p may be a sufficiently accurate description of many potentially useful barrier profiles (see also Ref [5]).

‡More precisely, this critical temperature depends on the density of dislocations, rather than on the plastic strain.

expected to decrease with increasing temperature, $a(T)$ is expected to be a decreasing function of temperature. For application to OFHC Cu, it turns out that $a(T)$ may be chosen to have the following simple form:

$$a(T) = a_0[1 - (T/T_m)^2], \tag{8c}$$

where T_m is the melting temperature ($\approx$1350 K, for copper), and a_0 depends on the initial average dislocation spacing. For the annealed samples, we expect that a_0 should be an order of magnitude greater than that for the as-received samples. We consider a_0 as an adjustable parameter to be fixed empirically. In the OFHC Cu case, $a_0 = 20$ for the annealed samples, and $a_0 = 1.8$ for the as-received samples, fit all our experimental data; see Section 4.

For the OFHC Cu, we approximate l by equation (8b), with $a(T)$ given by (8c). Expression (7) suggests that n_0 may be taken equal to 1/2. While, in general, we treat n_0 as a free constitutive parameter, for application to OFHC cooper, $n_0 = 1/2$ seems to fit the experimental data well, as is shown in Section 4. Hence, for this application, we choose

$$l = l_0/(1 + a(T)\gamma^{1/2}), \quad a(T) = a_0[1 - (T/T_m)^2]. \tag{8d}$$

Returning to the more general expressions (8a), note that equation (6) may now be written as

$$\hat{\tau} = \tau^0 f(\gamma, T), \quad \tau^0 = \frac{G_0}{b\lambda l_0}. \tag{9}$$

Note that τ^0 is inversely proportional to the initial average dislocation spacing, l_0. Its value, therefore, is expected to decease when an as-received sample is annealed. Indeed, for the OFHC Cu, we have found that $\tau^0 = 400$ MPa for the as-received samples, and $\tau^0 = 46$ MPa for the annealed samples, fit our experimental results. We note that, a_0 in equation (8c) and τ^0 in equation (9) are the only constitutive parameters that take on different values for the annealed and as-received OFHC Cu samples. All other parameters are kept the same over the entire range of strain rates from 10^{-3} to 8000 s^{-1} and temperatures from 77 to 1100 K, with strains up to 100%.

From equation (3), it is seen that $\dot{\gamma}_r$ for dislocations as barriers is also dependent on the dislocation density, being proportional to the average dislocation spacing, $d = l$. We thus assume that

$$\dot{\gamma}_r = \frac{\dot{\gamma}_0}{f(\gamma, T)}, \quad \dot{\gamma}_0 = b\rho_m\omega_0 l_0, \tag{10}$$

where l_0 is the initial average dislocation spacing. Hence, for dislocations as barriers,

$$\ln\frac{\dot{\gamma}}{\dot{\gamma}_r} = \ln\frac{\dot{\gamma}}{\dot{\gamma}_0} + \ln f(\gamma, T). \tag{11}$$

Combining equations (9) and (11), and in view of equation (7), the thermal part of the flow stress, τ^*, when the dislocations are the barriers to the motion of other dislocations, becomes

$$\tau^*(\gamma, \dot{\gamma}, T) = \tau^0\left\{1 - \left(-\frac{kT}{G_0}\left(\ln\frac{\dot{\gamma}}{\dot{\gamma}_0} + \ln f(\gamma, T)\right)\right)^{1/q}\right\}^{1/p} \times f(\gamma, T) \quad \text{for } T \le T_c \tag{12}$$

with $\tau^* = 0$ for $T > T_c$. Note that, in this case, the critical temperature, T_c, at which the dislocations as barriers cease to be significant, is dependent on the plastic strain, γ. This temperature is given by the relevant root of

$$T_c = -\frac{G_0}{k}\left[\ln\frac{\dot{\gamma}}{\dot{\gamma}_0} + \ln f(\gamma, T_c)\right]^{-1}. \tag{13}$$

2.2. *Effect on long-range barriers*

The athermal part, τ_a, of the flow stress, τ, represents the resistance to the motion of dislocations, provided by the potential fields of all other dislocations, grain boundaries, and defects. A dislocation must overcome this resistance through the applied resolved shear stress. This was recognized by Taylor [17] who noted that workhardening can result from the interaction between nonintersecting dislocations. Considerations of this kind suggest that the athermal stress, τ_a, may be taken as a function of the plastic strain, γ, as well as a function of the average grain size, d_G, and other parameters which represent the overall microstructural inhomogeneities†. Based on this observation, it may thus be reasonable to write

$$\tau_a = g(\gamma, d_G, \ldots)\tau_a^0, \tag{14}$$

where τ_a^0 has the dimensions of stress, and g is a dimensionless function of the indicated arguments. For example, it may be assumed that‡ .

$$\tau_a = \left(a_1 + \gamma^{n_1} + k_0 d_G^{-1/2}\right)\tau_a^0, \tag{15}$$

where a_1, n_1 and k_0 are constants.

2.3. *Final constitutive relation and estimate of parameters*

From equations (10) and (14), the final constitutive relation now becomes

$$\tau(\dot{\gamma}, \gamma, T) = \tau^0\left\{1 - \left(-\frac{kT}{G_0}\left(\ln\frac{\dot{\gamma}}{\dot{\gamma}_0} + \ln f(\gamma, T)\right)\right)^{1/q}\right\}^{1/p} \times f(\gamma, T) + \tau_a^0 g(\gamma, d_G, \ldots), \quad \text{for } T \le T_c. \tag{16}$$

For $T > T_c$, the flow stress is given by equation (14). As commented on before, we choose $q = 2$ and $p = 2/3$, and set $f(\gamma, T) = 1 + a(T)\gamma^{1/2}$, with the function $a(T)$ defined by equation (8c). Further, we

†It should be noted, however, that it is the *current density* of the dislocations, ρ_c, and not the accumulated plastic strain, γ, which directly affects τ_a; ρ_c, in general, will depend on the temperature history.

‡With $n_1 = 1/2$, this is the form used by Zerilli and Armstrong [18].

neglect the grain-size effects, and set $\tau_a = \tau_a^0 \gamma^{n_1}$, evaluating the free parameters empirically by comparison with the experimental results at suitably high temperatures. With these assumptions, the final constitutive relation becomes, for $T \leq T_c$,

$$\tau(\dot{\gamma}, \gamma, T) = \tau^0 \left\{ 1 - \left(-\frac{kT}{G_0} \left(\ln \frac{\dot{\gamma}}{\dot{\gamma}_0} + \ln\left(1 + a(T)\gamma^{1/2}\right)\right)\right)^{1/2} \right\}^{3/2} \left(1 + a(T)\gamma^{1/2}\right) + \tau_a^0 \gamma^{n_1}$$

$$\tau^0 = \frac{G_0}{b\lambda l_0}, \quad \dot{\gamma}_0 = b\rho_m \omega_0 l_0, \quad a(T) = a_0[1 - (T/T_m)^2]. \tag{17}$$

With $a_0 = 0$ and $l_0 = b$, this constitutive relation reduces to the expression developed for commercially pure tantalum by Nemat-Nasser and Isaacs [3], leading to excellent correlation with a broad range of experimental data. As is shown in Section 4, equation (17) fits all our high and low strain-rate experimental results, for both annealed and as-received OFHC Cu samples, remarkably well.

At this stage, it may be instructive to estimate some of the constitutive parameters on the basis of the physics of the plastic flow. As a starting point, consider k/G_0 and with G_0 slightly less than 2 eV set $k/G_0 = 5 \times 10^{-5}$ K^{-1}. This is about twice the value used by Nemat-Nasser and Isaacs [3] for commercially pure tantalum, where the lattice stress field provides the barrier resistance. For a dislocation as a barrier, the core of the dislocation involves a few surrounding atoms, and hence it is expected to provide greater resistance. The actual value of k/G_0 will be established empirically, once other parameters are fixed. This results in $k/G_0 = 4.9 \times 10^{-5}$ K^{-1} for application to our data.

To estimate $\dot{\gamma}_0$, note that $b \approx 2 \times 10^{-8}$ cm, $\omega_0 = O(10^{11}$ s$^{-1})$, and if we assume that $\rho_m = O(10^{11}$ cm$^{-2})$ and l_0 is about 500 lattice spacings, then it follows that $\dot{\gamma}_0 \approx 2 \times 10^{10}$ s^{-1}. We shall use this value for $\dot{\gamma}_0$, and adjust k/G_0 empirically, leading to $k/G_0 = 4.9 \times 10^{-5}$ K^{-1}. In this estimate, the value of ω_0 is that which has been suggested and justified by Kocks *et al.* ([5], p. 124).

Table 1 summarizes the values of the constitutive parameters, for both the annealed and as-received OFHC Cu samples, as well as for the commercially pure tantalum. As is seen, many of the parameters have essentially the same values. The basic differences stem from the difference between the spacing of the barriers, l. In the case of the commercially pure tantalum, it is assumed that the lattice is the only source of resistance to the motion of dislocations. In this case, l is of the order of the lattice spacing, i.e. $l \approx b$. It is for this reason that $\dot{\gamma}_0$ for copper is about two orders of magnitude greater than that for tantalum. The difference between the annealed and the as-received copper samples is also due to the difference in the initial dislocation spacing.

The formulation presented above does not include the effect of possible viscous drag on the motion of dislocations. At very high strain rates, the viscous drag may become dominant (see, e.g. Refs [5, 6, 9] and references cited therein). For a linear viscous drag resistance, the basic Equation (3) is simply modified as follows:

$$\frac{\dot{\gamma}}{\dot{\gamma}_0} = \frac{(1+\lambda')\tau^*}{\tau_D^0} \left\{ 1 + \frac{\tau^*}{\tau_D^0} \exp \Delta G/kT \right\}^{-1},$$

$$\tau_D^0 = \omega_0 D d/b \tag{18}$$

where D is the drag coefficient, and $\lambda' = \lambda/d$. Here, τ_D^0 is the reference drag stress. As is shown in the next section, for strain rates of up to 8000 s^{-1}, the inclusion of the drag forces does not seem necessary.

3. EXPERIMENTAL METHOD

The split Hopkinson bar has been used to obtain the inelastic response of metals, over a broad range of strain rates. The instrument is Kolsky's invention [19], based on the technique developed by John Hopkinson [20] and his son, Bertram Hopkinson [21, 22], who, respectively, used a single wire and a single rod to measure the dynamic tensile strength of the wire and the elastic stress pulse in the rod, under impact loads.

To relate the microstructural changes to the loading history, it is necessary to control the experiments such that the sample is subjected to only a given stress pulse and then is recovered, without having been subjected to any additional loads. This is accomplished using the modified Hopkinson procedure developed by Nemat-Nasser *et al.* [1] (1991). In the compression test, the recovery is accomplished through a construction which either traps or renders tensile all reflected pulses which travel toward the sample, once the initial compressive loading of the sample is completed. The mechanism

Table 1. Values of various constitutive parameters for annealed and as-received OFHC copper, and for commercially pure tantalum

Parameter	p	q	k/G_0	$\dot{\gamma}_0$	a_0	τ^0	τ_a^0	n_1
Annealed Cu	2/3	2	4.9×10^{-5} K^{-1}	2×10^{10} s^{-1}	20	46 MPa	220 MPa	0.3
As-received Cu	2/3	2	4.9×10^{-5} K^{-1}	2×10^{10} s^{-1}	1.8	400MPa	220 MPa	0.3
Tantalum	2/3	2	8.62×10^{-5} K^{-1}	5.46×10^{8} s^{-1}	0	1100 MPa	473 MPa	0.2

that is used to trap the incoming tensile pulse, has also been used to change (increase or decrease by about 30%) the strain rate during the compression loading at high strain rates; see, Nemat-Nasser *et al.* (1994) [2]. A similar change in the strain rate can be accomplished in UCSD's tension recovery Hopkinson technique.

Recently, Nemat-Nasser and Isaacs [3] have described a further enhancement of the compression recovery Hopkinson technique which allows measurement of the isothermal flow stress of certain metals over a broad range of temperatures and strain rates. For high-temperature tests, a furnace is employed to preheat the specimen while keeping the transmission and incident bars in the Kolsky split-bar construction of the Hopkinson technique [3], outside the furnace. These bars are then automatically brought into gentle contact with the specimen, just before the stress pulse reaches the specimen-end of the incident bar. Incremental straining is used to measure the strain softening produced by the temperature rise associated with the high strain-rate plastic deformation of the sample. The effect of any recovery on the flow stress that may occur during unloading, cooling to room temperature, reheating to the initial temperature, and reloading the sample, is assessed by overlapping the incremental straining of similar samples of the material. Since the basic technique is discussed and illustrated by Nemat-Nasser and Isaacs [3], only the results of the experiments on OFHC Cu samples are presented here and compared with the model predictions.

Experiments are performed on both annealed and as-received OFHC Cu samples, over the temperature range from 77 to 1100 K, at strain rates from 0.001 to 8000 s^{-1}, achieving strains of 100% and greater. The quasi-static tests are performed using an Instron machine. The test results are presented in the next section together with the corresponding theoretical predictions.

4. RESULTS AND DISCUSSION

The high-temperature results can be used to fix the constitutive parameters, n_1 and τ_a^0, which define the athermal part of the flow stress in Equation (17). Since heating a sample to high-temperatures automatically anneals it, the high temperature results should be independent of the initial condition of the sample, i.e. whether it is annealed or workhardened. The experimental results support this observation. Indeed, repeated incremental loading of a sample at 600 K and greater initial temperature, reproduces the same stress–strain relationship, as is illustrated in Fig. 1, for a 696 K initial temperature and 4000 s^{-1} strain rate. The curves shown in this figure are obtained by straining the sample by about 28% true strain and then allowing the sample to cool to room temperature, before it is reheated to the same initial temperature of 696 K and then

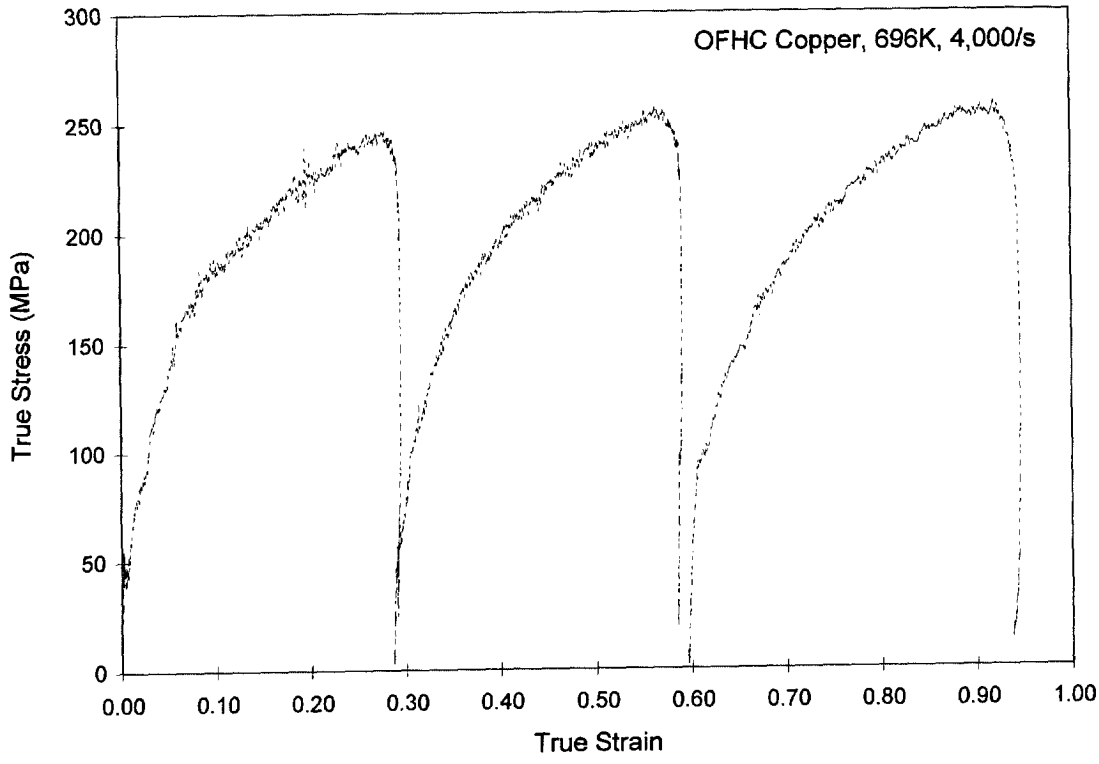

Fig. 1. Stress–strain relationships for an OFHC copper sample which has been tested incrementally at 696 K initial temperature and 4000 s^{-1} strain rate; note that the three curves are essentially the same.

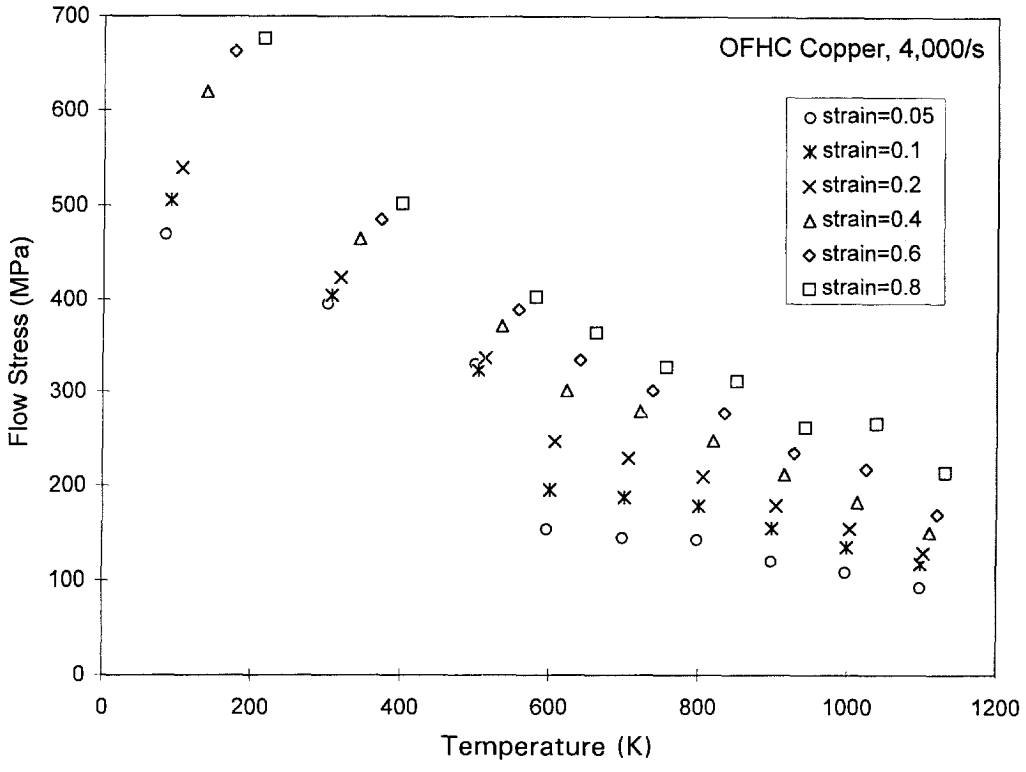

Fig. 2. Experimentally obtained flow stresses for as-received OFHC copper at 4000 s^{-1} strain rate and indicated constant strains, as functions of absolute temperature; note the tendency of the curves towards limiting, athermal values (see Fig. 3).

re-strained by an additional 30% strain increment at the same strain rate of 4000 s^{-1}. The three curves are essentially the same and almost coincide with one another if they are translated to a common origin. Thus, the sample in each of these incremental loadings should be viewed as a virgin and annealed one. Except for a translation along the strain axis, the constitutive relation (17) should fit all three curves whether the parameters for the annealed or those for the as-received cases are used.

To obtain the initial estimates of the constitutive parameters, we have first followed the procedure outlined by Nemat-Nasser and Isaacs [3], and plotted the experimentally obtained flow stress as a function of the absolute temperature, for fixed strains and the constant strain rate of 4000 s^{-1}. Figure 2 shows these results for the as-received material. As is seen, the curves tend to limiting values which are independent of the temperature. These limiting values fit a simple power law (see Fig. 3),

$$\tau_a = 208\ \gamma^{0.27}, \tag{19}$$

suggesting that†, in equation (15), $a_1 \approx 0$, $\tau_a^0 \approx 210$ MPa and $n_1 \approx 0.3$. It turns out that $\tau_a^0 = 220$ MPa fits the data slightly better. Hence $n_1 = 0.3$ and $\tau_a^0 = 220$ MPa are the values listed in Table 1.

As pointed out before, $k/G_0 = 4.9 \times 10^{-5}$ K^{-1} and $\dot{\gamma}_0 = 2 \times 10^{10}$ s^{-1} are suitable values for OFHC Cu, both for annealed and as-received samples. The remaining parameters in equation (17) are τ_0 and a_0. Examination of the experimental results reveals that $\tau_0 = 400$ MPa and $a_0 = 1.8$ for the as-received material and $\tau_0 = 46$ MPa and $a_0 = 20$ for the annealed material fit all our experimental data. Since τ^0 is inversely proportional to the initial average dislocation spacing, l_0, [see equation (17)], we expect such a difference in the value of τ^0. Also, we expect the average dislocation spacing to decrease at a greater rate with plastic straining, when the sample is annealed. This is reflected by the difference in the values of a_0 for the as-received and annealed cases.

Figures 4–7 compare the model predictions with the experimental curves. The first two figures are for the as-received samples, whereas the second two are for the annealed samples. Only the samples tested at low temperatures were pre-annealed. As pointed out before, for initial temperatures of

†It turns out that the model is not too sensitive to the exact values of the parameters which best fit the experimental data. For this reason, we round all the parameters to within 10%, using instead of, say, $n_1 = 0.27$, the rounded values of $n_1 = 0.3$. In general, the accuracy of the experimental evaluation of the flow stress of metals, does not warrant more accurate estimates of the model parameters.

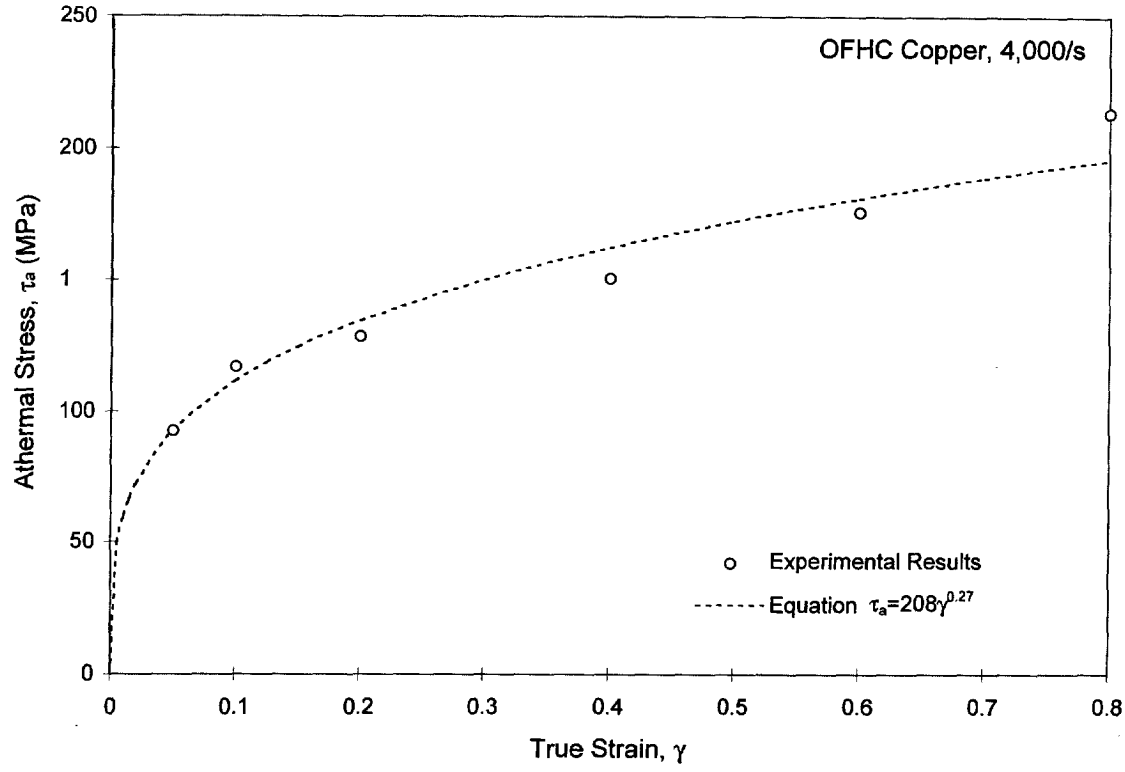

Fig. 3. Athermal stress as a function of strain for OFHC copper at 4000 s^{-1} strain rate.

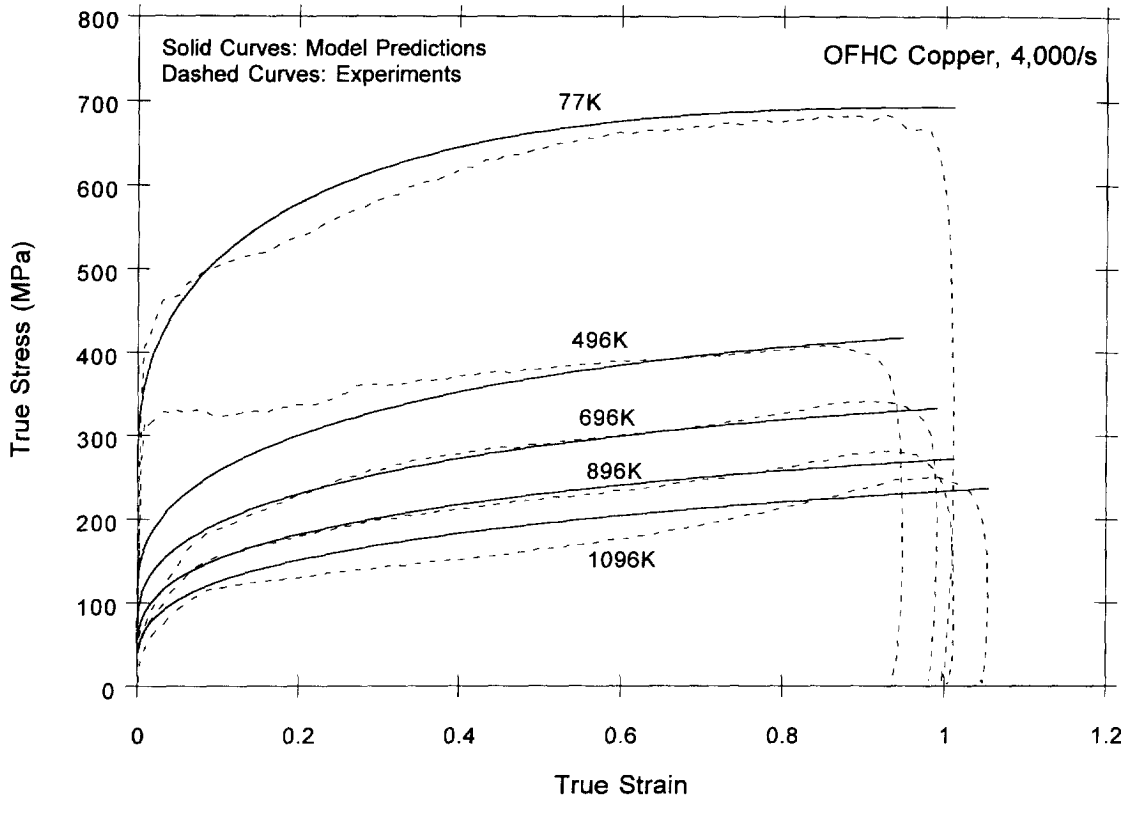

Fig. 4. Comparison of model predictions with experimental results for as-received OFHC copper at 4000 s^{-1} strain rate and indicated temperatures (see also Fig. 5).

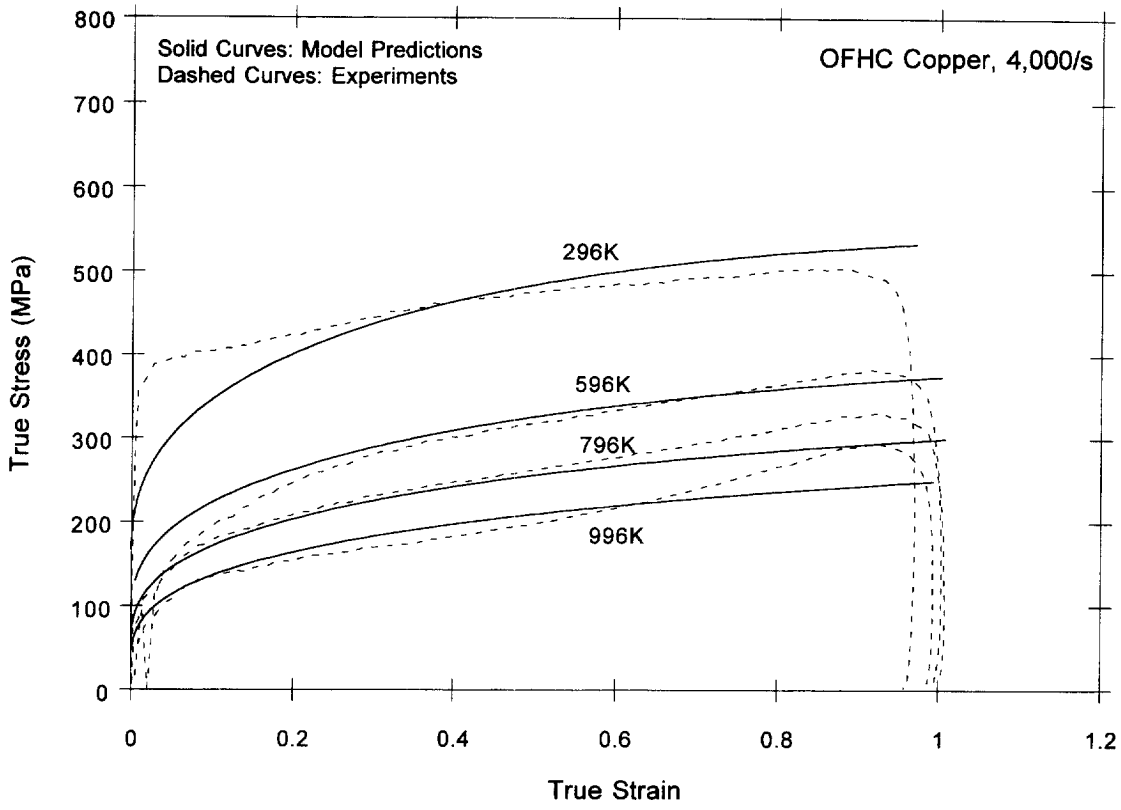

Fig. 5. Comparison of model predictions with experimental results for as-received OFHC copper at 4000 s^{-1} strain rate and indicated temperatures (see also Fig. 4).

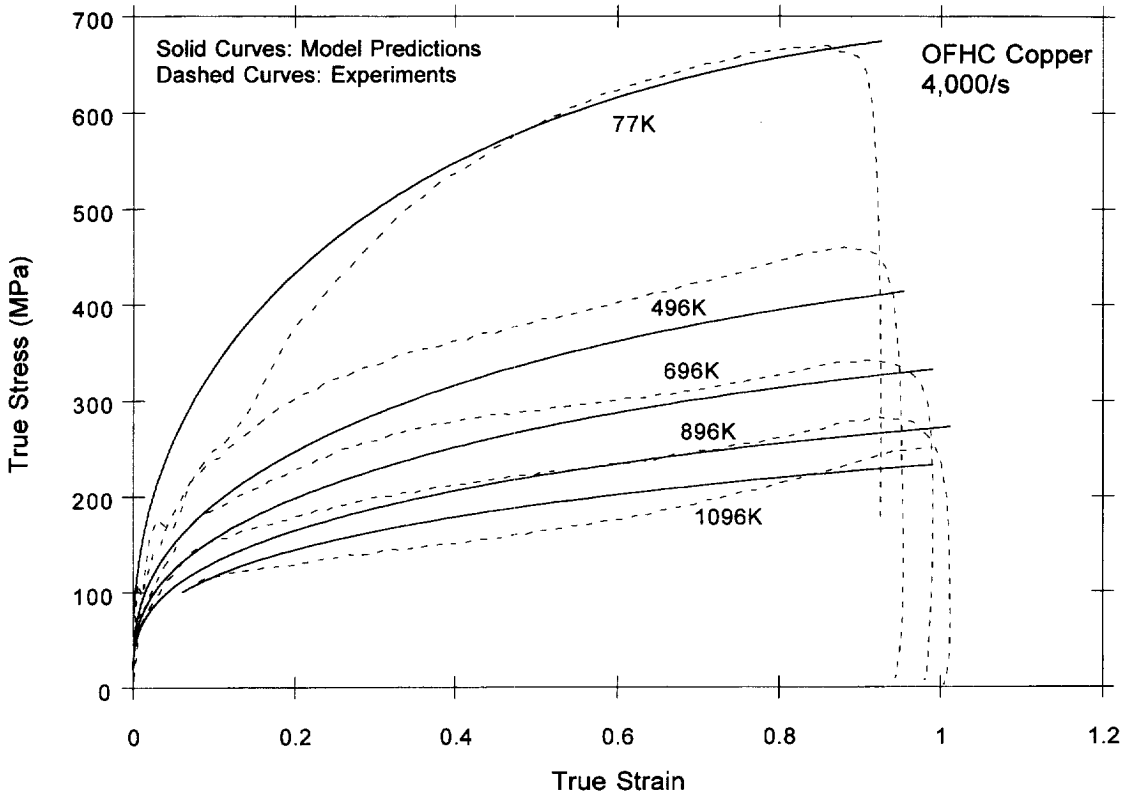

Fig. 6. Comparison of model predictions with experimental results for annealed OFHC copper at 4000 s^{-1} strain rate and indicated temperatures (see also Fig. 7).

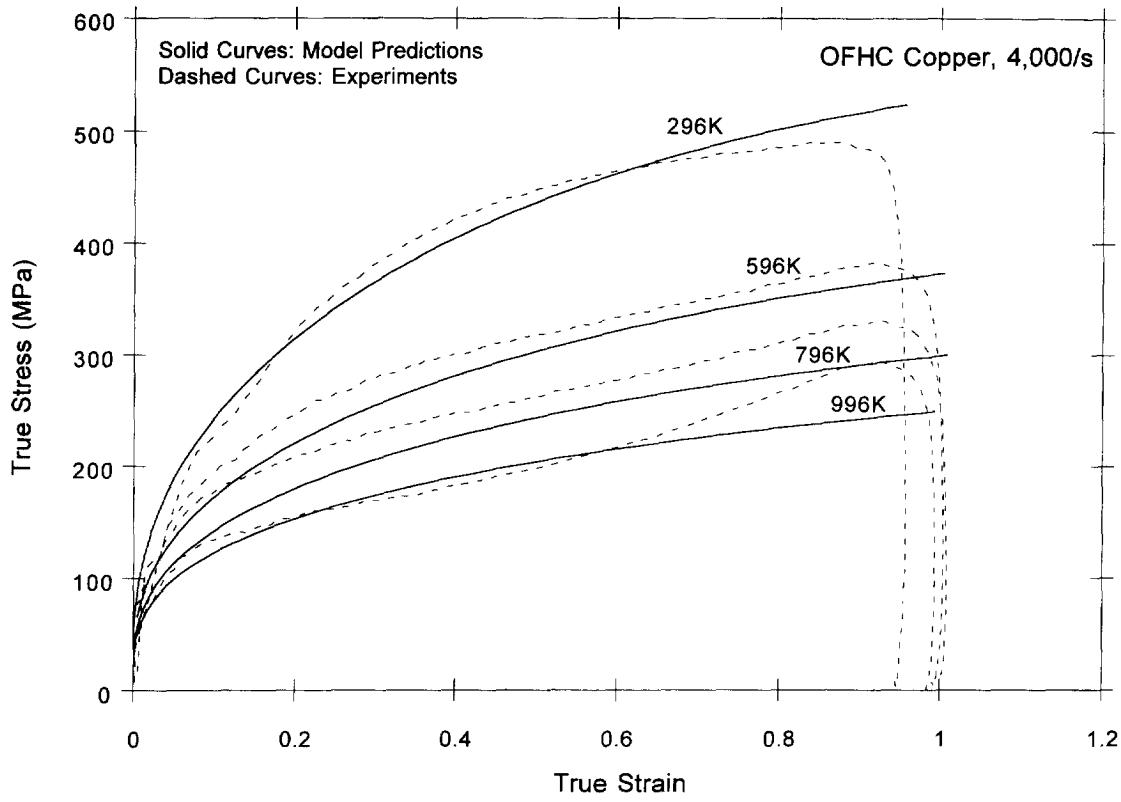

Fig. 7. Comparison of model predictions with experimental results for annealed OFHC copper at 4000 s^{-1} strain rate and indicated temperatures (see also Fig. 6).

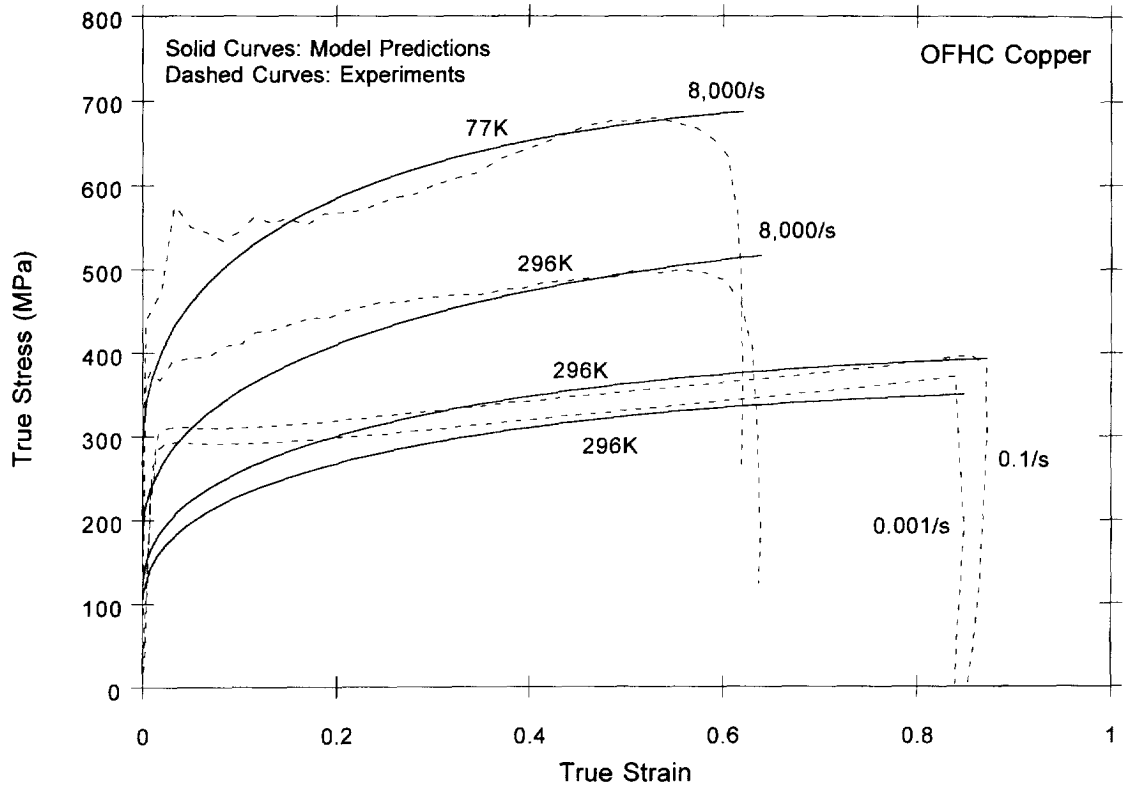

Fig. 8. Comparison of model predictions with experimental results for as-received OFHC copper at indicated strain rates and temperatures.

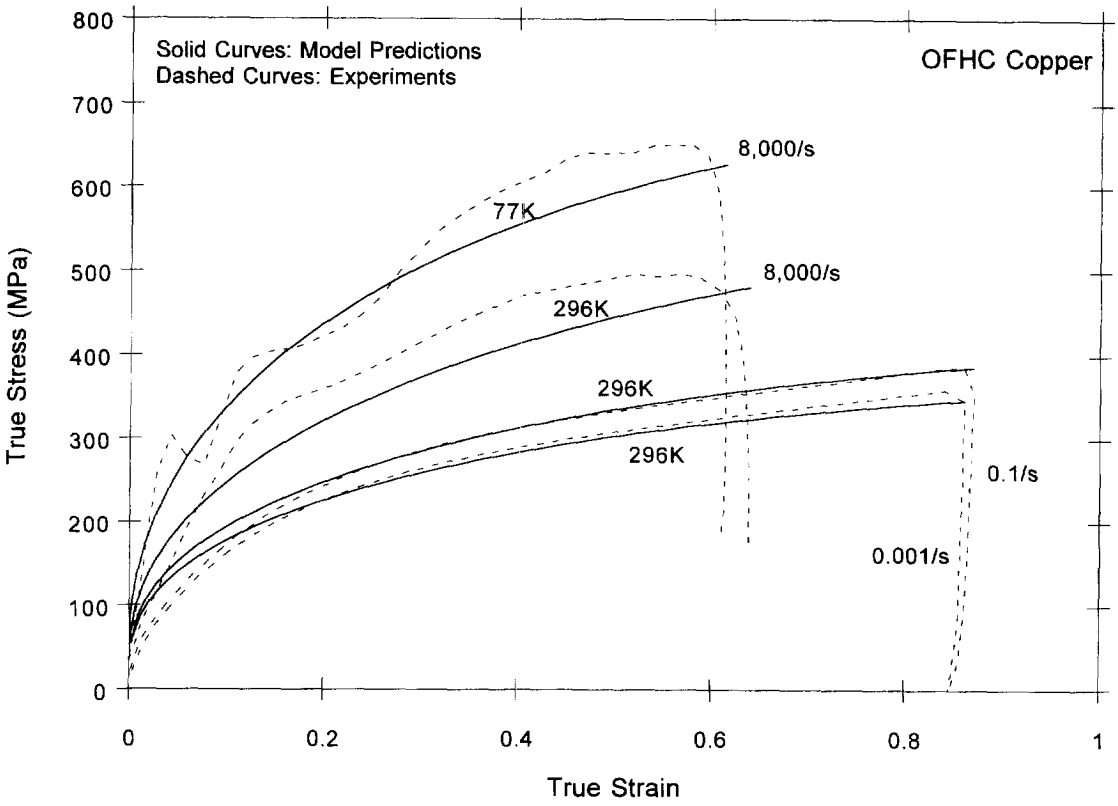

Fig. 9. Comparison of model predictions with experimental results for annealed OFHC copper at indicated strain rates and temperatures.

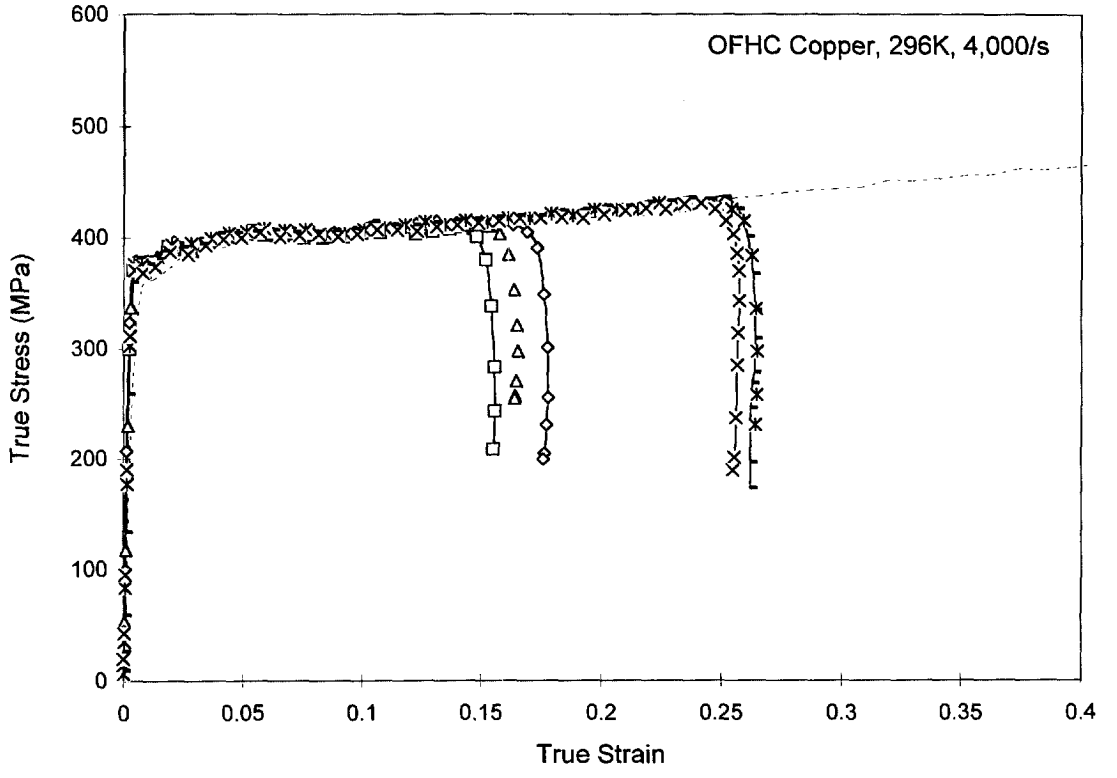

Fig. 10. Comparison of six different tests of the as-received OFHC copper samples at 4000 s^{-1} strain rate and room temperature, showing the repeatability of the experiments.

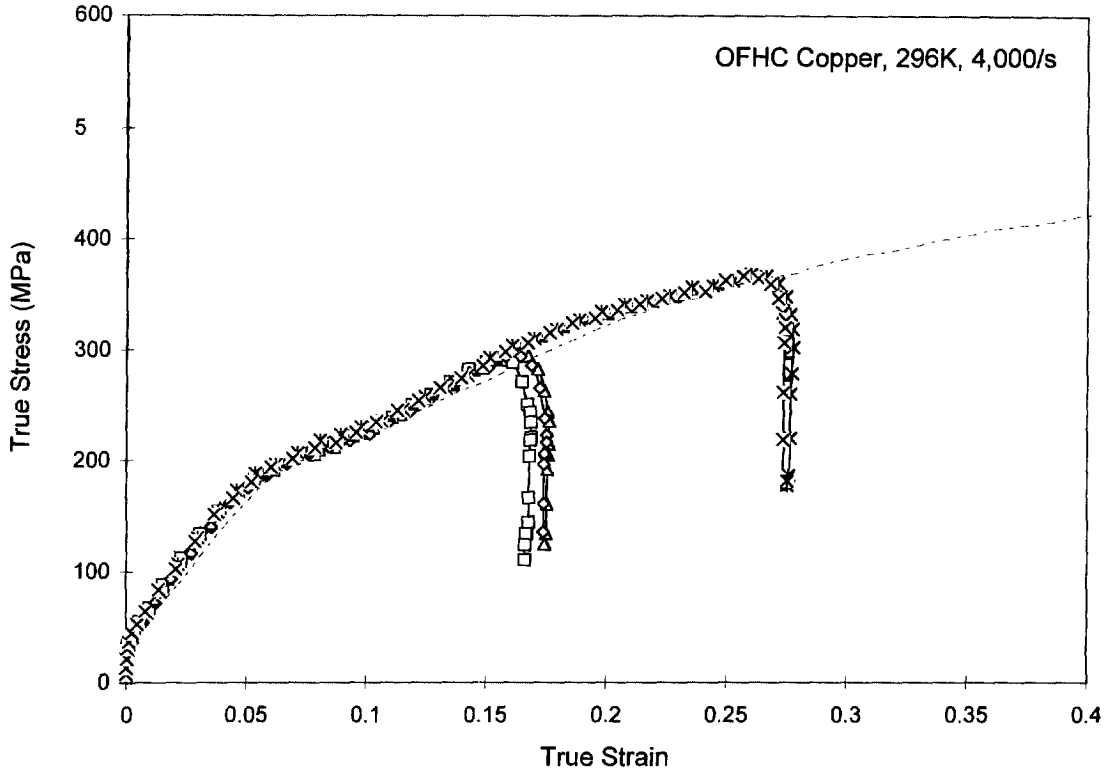

Fig. 11. Comparison of six different tests of the annealed OFHC copper samples at 4000 s^{-1} strain rate and room temperature, showing the repeatability of the experiments.

696 K and greater, the sample anneals while it is being brought to the required temperature in the furnace. As is seen, *the model fits these data, whether the parameters for the annealed or those for the as-received cases are used.*

In addition, we have performed experiments at 8000 s^{-1} strain rate and initial temperatures of 77 and 296 K, for both the as-received and annealed samples. These are shown in Figs 8 and 9 which also include the quasi-static results obtained at room temperature. The theoretical results are shown by the solid curves in these figures. Both the high-strain-rate and low-strain-rate predictions are quite good. While it is possible to further tune the constitutive parameters to better fit all cases, this is deemed unwarranted, considering the broad range of temperatures and strain rates for which the fit is, in fact, quite good.

Finally, we have checked the repeatability and quality of our tests and the test procedure, by performing independent tests on similar samples at the same strain rate (4000 s^{-1}) and initial temperature (room) but using different strain increments. These are shown in Figs 10 and 11, for as-received and annealed samples. As is seen, the results are essentially indistinguishable, indicating the quality of the the procedure and the test results.

Acknowledgements—The authors would like to thank Mr. J Isaacs for his assistance in performing the experiments. The work reported here has been supported by the Army Research Office under contract No. DAAL03-92-G-0108 with the University of California, San Diego.

REFERENCES

1. Nemat-Nasser, S., Isaacs, J. B. and Starrett, J. E., *Proc. R. Soc.*, 1991, **435A**, 371.
2. Nemat-Nasser, S., Li, Y. F. and Isaacs, J. B., *Mech. Mater.*, 1994, **17**, 111.
3. Nemat-Nasser, S. and Isaacs, J. B., *Acta Metall.*, 1997, **45**, 907.
4. Gilman, J. J., *Micromechanics of Flow in Solids*, McGraw-Hill, NY, 1969.
5. Kocks, U. F., Argon A. S. and Ashby, M. F., *Progress in Materials Science. Thermodynamics and Kinetics of Slip*. Vol. 19. Pergamon, Oxford. 1975.
6. Clifton, R. J., *J. Appl. Mech.*, 1983, **50**, 941.
7. Follansbee, P. S., *Metallurgical Applications of Shock-wave and High-strain Rate Phenomena*, ed. L. E. Murr, K. P. Staudhammer and M. A. Meyers. Marcel Dekker. 1986, 451–479.
8. Klepaczko, J. R. and Chiem, C. Y., *J. Mech. Phys. Solids.*, 1986, **34**, 29.
9. Regazzoni, G., Kocks, U. F. and Follansbee, P. S., *Acta Metall.*, 1987, **35**, 2865.
10. Follansbee, P. and Kocks, U. F., *Acta Metall.*, 1988, **36**, 81.
11. Follansbee, P. S. and Gray, G. T., *Int. J. Plasticity*, 1991, **7**, 651.
12. Weertman, J. and Weertman, J. R., *Elementary Dislocation Theory*, Macmillan, 1964.

13. Hirth, J. P. and Lothe, J., *Theory of Dislocations*, Krieger, Malabar, FL, USA, 1992.
14. Hull, D. and Bacon, D. J., *Introduction to Dislocations*. Pergamon, Oxford, 1984.
15. Ono, K., *J. Appl. Phys.*, 1968, **39**, 1803.
16. Johnson, G. R. and Cook, W. H., *Proc. 7th Int. Symp. on Ballistics*, The Hague, Netherlands, 1983, 1–7.
17. Taylor, G. I., *Proc. R. Soc.*, 1934, **145A**, 362.
18. Zerilli, F. J. and Armstrong, R. W., *J. Appl. Phys.*, 1987, **61**, 1816.
19. Kolsky, H., *Proc. Roy. Soc.*, 1949, **62**, 676.
20. Hopkinson, J., *Proc. Manchester Literary & Philos. Soc.*, 1872, **XI**, 40.
21. Hopkinson, B., *Proc. Roy. Soc.*, 1905, **74**, 498.
22. Hopkinson, B., *Phil. Trans. A*, 1914, **213**, 437.